THREE DIMENSIONAL COUPLED SIMULATION OF FURNACES AND REACTOR TUBES FOR THE THERMAL CRACKING OF HYDROCARBONS

T. DETEMMERMAN and F. FROMENT

Laboratorium voor Petrochemische Techniek[1]

SIMULATION TRIDIMENSIONNELLE ET COUPLÉE DES FOURS ET DES TUBES DE RÉACTEURS POUR LE CRAQUAGE THERMIQUE DES HYDROCARBURES

Le craquage thermique des hydrocarbures a évolué d'une manière significative au cours des 20 dernières années. Des progrès dans les métallurgies associés à une meilleure compréhension des mécanismes de réaction ont conduit à de nouvelles configurations pour les fours et les réacteurs qui s'orientent toutes vers des conditions de craquage plus sévères. Une modélisation directe et tridimensionnelle comprenant des équations de transport de masse, de moment et d'énergie a été implantée dans le code FLOWSIM, en même temps que le modèle k-ε de turbulence. Cette modélisation a été couplée avec les modèles cinétiques appropriés (le schéma CRACKSIM pour les réactions radicalaires dans le réacteur et les cinétiques de combustion dans le four) et un schéma itératif global a été développé pour la simulation couplée four-réacteur permettant de simuler des unités industrielles. Cette approche a été appliquée à un four de craquage pour le propane, apportant une compréhension détaillée des mécanismes de transport qui s'y déroulent.

THREE DIMENSIONAL COUPLED SIMULATION OF FURNACES AND REACTOR TUBES FOR THE THERMAL CRACKING OF HYDROCARBONS

Thermal cracking of hydrocarbons has gone through a significant evolution over the past 20 years. Improved metallurgical properties together with a better understanding of the chemical aspects have led to new configurations for furnace and reactor, all aiming for high severity cracking. A full 3D CFD model containing transport equations for mass, momentum and energy has been implemented in the software code FLOWSIM, together with the k-ε turbulence model. It has been coupled with the appropriate kinetic models (the radical reaction scheme CRACKSIM for the reactor and combustion kinetics for the furnace) and an overall iteration scheme has been developed for a coupled furnace-reactor simulation allowing to simulate industrial units. This approach has been applied for a propane cracking furnace, providing detailed understanding of the transport mechanisms taking place.

(1) Universiteit Gent,
Krijgslaan 281, B9000 Gent - Belgium

SIMULACIÓN TRIDIMENSIONAL Y ACOPLADA DE LOS HORNOS Y DE LOS TUBOS DE REACTORES PARA EL CRAQUEO TÉRMICO DE LOS HIDROCARBUROS

El craqueo térmico de los hidrocarburos ha evolucionado de forma significativa durante el transcurso de los veinte últimos años. Los progresos en las metalurgias asociadas han conducido a nuevas configuraciones para los hornos y los reactores que, todas ellas, se orientan hacia nuevas configuraciones en condiciones de craqueo de mayor severidad. Una modelización directa y tridimencional que incluye ecuaciones de tranferencia de masa, de momento y de energía ha sido implantada en el código FLOWSIM, al mismo tiempo que el modelo k-ε de turbulencia. Se ha acoplado esta modelización con los modelos cinéticos adecuados (el esquema CRACKSIM para las reacciones radicalares en el reactor y las cinéticas de combustión en el horno) y, asimismo, se ha desarrollado un sistema iterativo global para la simulación en acoplamiento horno-reactor que permite simular las unidades industriales. Se ha aplicado este enfoque a un horno de craqueo para el propano, que ha permitido una comprensión detallada de los mecanismos de transferencia que en él se desarrollan.

INTRODUCTION

Olefins, the major building blocks for the petrochemical industry, are mainly produced by the thermal cracking of hydrocarbons in tubular reactors suspended in large, gas fired furnaces. The technology of thermal cracking has gone through a significant evolution during the last 20 years. Improved metallurgical properties combined with a better understanding of the chemical aspects have led to new configurations for the reactor and for the furnace. These aim for high severity cracking, involving shorter residence times, increased heat fluxes and higher temperatures. In this paper a simulation procedure is discussed for a propane cracking unit with a very short residence time of the process gas in the reactor.

The zone method of Hottel and Sarofim (1967) is used for the simulation of the heat transfer in the furnace. This simulation method was developed by Vercammen and Froment (1978, 1980), Rao *et al*. (1988) and Plehiers and Froment (1989). The radiative heat transfer is calculated by means of a Monte Carlo method. To meet the present requirements for the simulation of thermal cracking units, the flue gas flow patterns in the firebox have to be taken into account. Modern computer capacities allow a prediction of this flow pattern based on well established CFD techniques using turbulence models. The flue gas concentration profiles have to be calculated from continuity equations for all flue gas species. The fuel gas disappearance is not only determined by the rate of the combustion reaction. The fuel gas components have to be intimately mixed before combustion can take place. This is taken into account by means of an eddy break up model. Finally, the furnace calculations have to be coupled with a reactor tube simulation. For new types of reactors with internal helicoidal fins, the classical and widely used one-dimensional plug flow model is no longer satisfactory. The flow pattern and the product yields have to be calculated from a full, three dimensional reactor model.

1 DESCRIPTION OF THE CRACKING UNIT

In the cracking unit (Fig. 1), four sections can be distinguished: the radiation section, the cross over section, the convection section and the quenches. The radiation section contains 160 reactor tubes on one row in the center plane of the furnace. Each tube has

internal, helicoidal fins and makes one pass through this section. After the radiation section the process gas flows through an adiabatic connection, uniting four reactor tubes, before going to the quenches.

The heat required for the endothermic cracking reactions is generated by means of burners located in the bottom plate of the furnace. These burners are rectangular boxes through which air flows, while the fuel gas, a mixture of methane and hydrogen coming from the demethanizer, is fed through a rectangular slit in the center of the box. The flue gas, leaving the radiation section at approximately 1100°C flows, via the cross-over section, to the convection section where heat is recovered. Several tasks are fullfilled here: preheating the feed water for the steam drum, production of dilution steam, preheating the reactor feed and superheating of steam. The process gas flows via an adiabatic connection to the quenches. The process gas is quenched with high pressure steam to avoid secondary reactions.

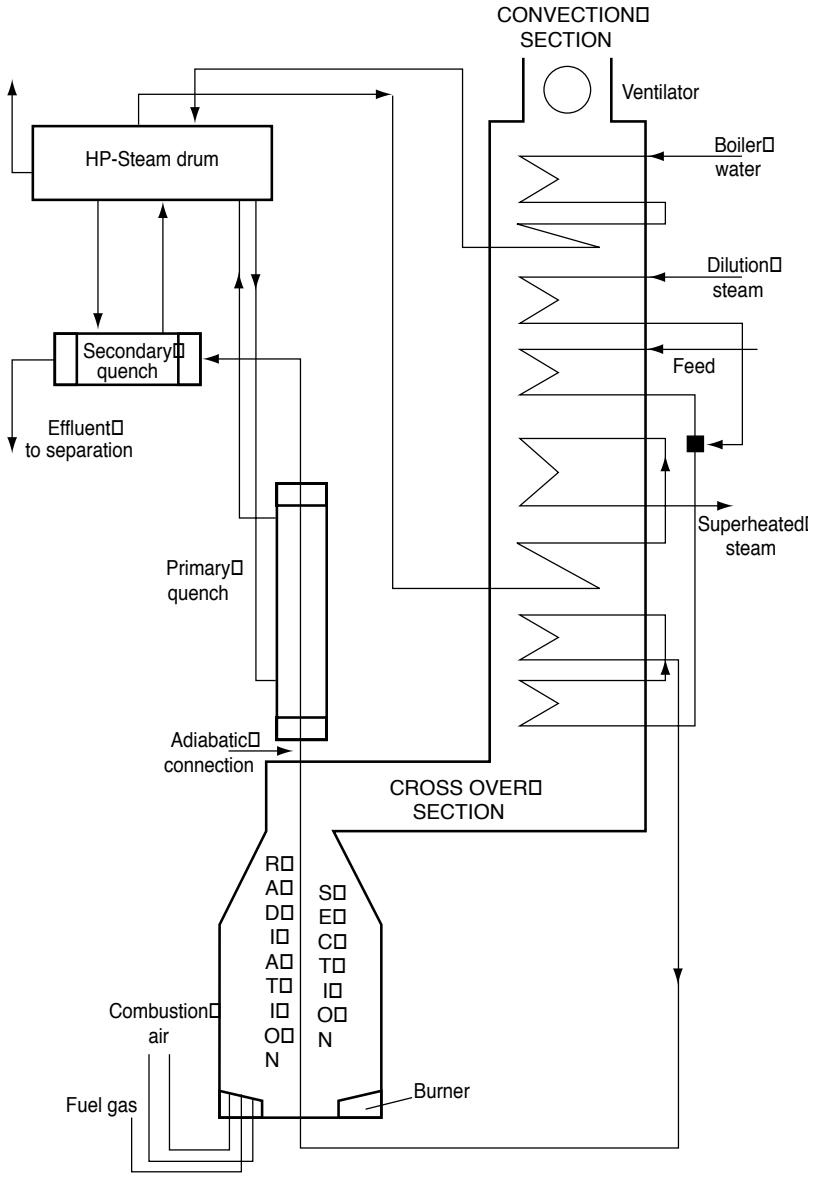

Figure 1

Schematic representation of the propane furnace.

2 SIMULATION MODEL

2.1 Zone method of Hottel for the furnace simulation

The furnace is divided into isothermal surface and volume zones. An energy balance is constructed for each zone, describing the heat exhange between the different zones. These energy balances for the zones lead to the following set of equations:

$$\begin{bmatrix} Z_1Z_1-\Sigma & Z_1Z_j & & Z_2Z_1 & \cdots & & Z_nZ_1 \\ & Z_1Z_2 & Z_2Z_2-\Sigma & Z_2Z_j & \cdots & & Z_nZ_2 \\ & . & & . & . & & . \\ & . & & . & . & & . \\ & Z_1Z_n & & Z_2Z_n & \cdots & Z_nZ_n-\Sigma & Z_nZ_j \end{bmatrix} \cdot \begin{bmatrix} E_1 \\ E_2 \\ . \\ . \\ E_n \end{bmatrix} = \begin{bmatrix} Q_1 \\ Q_2 \\ . \\ . \\ Q_n \end{bmatrix} \quad (1)$$

The matrix element Z_iZ_j is the total exchange area between the zones i and j. This is the amount of radiative heat emitted by zone i and absorbed by zone j, divided by the blackbody emissive power E_i:

$$E_i = \sigma \ T_i^4 \quad (2)$$

The total exchange areas are calculated from the view factors in a diathermal medium, by taking absorption of heat and reflection on the surface zones into account.

The view factors are determined from of a Monte Carlo method. Flue gas absorption is taken into account via the band model of Edwards. Reflection of heat is incorporated via a matrix algorithm developed by Hottel (Hottel and Sarofim, 1967). The determination of the total exchange areas was discussed in detail by Rao *et al.* (1988) and Plehiers and Froment (1989).

The Q_i in the right hand side of (1) contain the non-radiative contributions to the energy balances, such as the heat loss to the environment, the heat release by combustion, the flue gas convection and heat transfer by conduction and convection to the reactor process gas.

2.2 Calculation of the flue gas flow pattern

The flue gas flow pattern is calculated from a CFD model based on the Reynolds averaged Navier-Stokes equations containing:

- a total continuity equation:

$$\sum_{i=1}^{3} \frac{\partial}{\partial_{x_i}} \left(\rho_g U_i \right) = 0 \quad (3)$$

- a momentum equation in the i-direction (for i = 1 to 3):

$$\sum_{j=1}^{3} \frac{\partial}{\partial_{x_j}} \left(\rho_g U_j U_i \right) = -\frac{\partial p}{\partial_{x_i}} + \sum_{j=1}^{3} \frac{\partial}{\partial_{x_j}} \left(\mu_t \left(\frac{\partial U_i}{\partial_{x_j}} + \frac{\partial U_j}{\partial_{x_i}} \right) \right) \quad (4)$$

The left hand side of the momentum equations accounts for the convective transport of the i-th component of the momentum. The first term in the right hand side accounts for the pressure forces and the second term for the viscous forces due to velocity gradients. To take the influence of temperature variations on the flow pattern into account, an energy equation is included:

$$\sum_{i=1}^{3} \frac{\partial}{\partial_{x_i}} \left(\rho_g U_i \left(H + k + \varepsilon_k \right) \right) - \sum_{i=1}^{3} \sum_{j=1}^{N} \frac{\partial}{\partial_{x_i}} \left(\rho_g D_t \frac{\partial_{y_j}}{\partial_{x_i}} H_j \right) - \sum_{i=1}^{3} \frac{\partial}{\partial_{x_i}} \left(\lambda_t \frac{\partial T}{\partial_{x_i}} \right) = Q_{rad} \quad (5)$$

with

$$H = \sum_{j=1}^{N} y_j H_j ; \ e_k = \frac{1}{2} \sum_{i=1}^{3} U_i^2 \quad (6)$$

The left hand side of this equation, expressed in terms of enthalpy, consists of three terms: the first term indicates the convective transport of enthalpy, turbulent energy and kinetic energy; the second term expresses the interdiffusional enthalpy transport and the third term accounts for the turbulent heat conduction. Q_{rad} represents the radiation heat received per unit of volume. To take the local influence of radiation on the temperature distribution into account, the six flux model proposed by De Marco and Lockwood (1975) is used. In this model, a generalized distribution for the radiation intensity:

$$I = A_x \cdot \Omega_x + A_y \cdot \Omega_y + A_z \cdot \Omega_z + B_x \cdot \Omega_x^2 + B_y \cdot \Omega_y^2 + B_z \cdot \Omega_z^2 \quad (7)$$

is substituted into the integro-differential Equation describing this intensity:

$$\nabla \cdot (I \cdot \overline{\Omega}) = -k_g I + k_g \frac{\sigma T^4}{\pi} \tag{8}$$

This equation expresses that net changes in the radiation intensity are due to flue gas absorption and flue gas emission.

equations for the *A* and *B* coefficients are obtained by integration of (8) over six segments of the total solid angle 4π. Q_{rad} is calculated from:

$$Q_{rad} = \int_{4\Pi} \nabla \cdot (I\,\overline{\Omega})\, d\Omega \tag{9}$$

(5) can be transformed into (10) in which the heat of reaction explicitly appears in the right hand side.

$$\begin{aligned} &\sum_{i=1}^{3} \rho_g U_i \left(\frac{\partial}{\partial_{x_i}} (k + e_k) + C_p \frac{\partial T}{\partial_{x_i}} \right) \\ &- \sum_{i=1}^{3} \sum_{j=1}^{N} \frac{\partial}{\partial_{x_i}} \left(\rho_g D_t \frac{\partial_{y_j}}{\partial_{x_i}} H_j \right) \\ &= \sum_{i=1}^{3} \frac{\partial}{\partial_{x_i}} \left(\lambda_t \frac{\partial T}{\partial_{x_i}} \right) \\ &+ \sum_i (-\Delta H_i r_i) + Q_{rad} \end{aligned} \tag{10}$$

The viscosity μ_t, the conductivity λ_t and the diffusivity D_t are the sum of the corresponding molecular and turbulent properties:

$$\begin{aligned} \mu_t &= \mu_m + \mu_{turb} \\ \lambda_t &= \lambda_m + \lambda_{turb} \\ D_t &= D_m + D_{turb} \end{aligned} \tag{11}$$

The turbulent properties are calculated via the *k*-ε turbulence model in which turbulence is defined through the turbulent kinetic energy *k* and the dissipation rate of *k*, represented by ε. A conservation equation has to be included for *k* and ε:

$$\sum_{i=1}^{3} \frac{\partial}{\partial_{x_i}} (\rho_g U_i k) = \sum_{i=1}^{3} \frac{\partial}{\partial_{x_i}} \left(\mu_t \frac{\partial k}{\partial_{x_i}} \right) + P_k - \rho_g \varepsilon \tag{12}$$

$$\begin{aligned} \sum_{i=1}^{3} \frac{\partial}{\partial_{x_i}} (\rho_g U_i \varepsilon) &= \sum_{i=1}^{3} \frac{\partial}{\partial_{x_i}} \left(\frac{\mu_t}{1.33} \frac{\partial \varepsilon}{\partial_{x_i}} \right) \\ &+ P_e - 1.92\ \rho_g \frac{\varepsilon^2}{k} \end{aligned} \tag{13}$$

with

$$\begin{aligned} P_k &= \sum_{i=1}^{3} \sum_{j=1}^{3} \mu_t \left(\frac{\partial U_i}{\partial x_j} + \frac{\partial U_j}{\partial x_i} \right) \frac{\partial U_i}{\partial x_j} \\ P_\varepsilon &= 1.44 \frac{\varepsilon}{k} P_k \end{aligned} \tag{14}$$

The *k* equation can be derived from the Navier-Stokes equations. A conservation equation for ε can also be derived from the Navier-Stokes equations, but it contains too many unknown terms. Therefore, an empirical equation similar to the one for *k* is used in the standard *k*-ε model.

The turbulent viscosity μ_{turb} is calculated from the Prandtl-Kolmogorov expression:

$$\mu_{turb} = 0.09\ \rho_g \frac{k^2}{\varepsilon} \tag{15}$$

The turbulent conductivity λ_{turb} and diffusivity D_{turb} are obtained out of analogy (De Saegher *et al.*, 1996).

2.3 Calculation of the concentration profiles in the flue gas

Since the burners produce flames extending into the furnace, the simulation of the latter has to be considered as the combustion of the fuel gas components. For each flue gas component a continuity Equation is solved:

$$\sum_{i=1}^{3} \frac{\partial}{\partial_{x_i}} \left(\rho_g U_i y_j \right) = \sum_{i=1}^{3} \frac{\partial}{\partial_{x_i}} \left(\rho_g D_t \frac{\partial_{y_j}}{\partial_{x_i}} \right) + R_j M_j \tag{16}$$

At some stage, when the combustion is complete, the term $R_j M_j$ will vanish. The disappearance of methane and hydrogen is determined by two phenomena that occur sequentially.

Fuel gas and combustion air first have to be mixed turbulently before they can react. For the combustion reaction the following mechanism was assumed:

$$CH_4 + \frac{3}{2} O_2 \xrightarrow{1} CO + 2H_2O$$

$$CO + \frac{1}{2} O_2 \xrightarrow{2} CO_2$$

$$H_2 + \frac{1}{2} O_2 \xrightarrow{3} H_2O$$

and the kinetics proposed by Dryer and Glassman (1973) were applied:

$$r_{1,k} = 10^{7.2} \exp\left(-\frac{202600}{RT}\right) C_{CH_4}^{0.7} C_{O_2}^{0.8}$$
$$r_{2,k} = 10^{8.6} \exp\left(-\frac{167500}{RT}\right) C_{CO} C_{H_2O}^{0.5} C_{O_2}^{0.25} \quad (17)$$

The combustion of hydrogen is assumed to be infinitely fast. For the turbulent mixing, the eddy break up model proposed by Spalding (1972) was applied. The reaction mixture is assumed to exist out of eddies containing the pure reaction components. Due to turbulent mixing, these eddies are broken down to a level at which reaction is possible. When this eddy break up is slow, it can determine the overall rate of fuel gas consumption.

To obtain a mixing time scale τ_m, analogy is assumed between the eddy break up and the decay of turbulent kinetic energy, for which the following rate can be derived from the Navier Stokes Equations (Hinze, 1959):

$$\tau_m^{-1} = 4 \frac{\varepsilon}{k} \qquad [s^{-1}] \quad (18)$$

The following mixing rates are obtained for the various reactions:

$$r_{1,m} = 4\rho_g \frac{\varepsilon}{k} \min\left(y_{CH_4}, 0.33 y_{O_2}\right)$$
$$r_{2,m} = 4\rho_g \frac{\varepsilon}{k} \min\left(y_{CO}, 1.75 y_{O_2}\right) \quad (19)$$
$$r_{3,m} = 4\rho_g \frac{\varepsilon}{k} \min\left(y_{H_2}, 0.13 y_{O_2}\right)$$

Since the turbulent mixing and combustion occur sequentially, mixing and reaction times can be added up, leading to the following expressions for the overall rates:

$$r_{1,y} = \left\{\frac{1}{r_{1,k}} + \frac{M_{CH_4}}{r_{1,m}}\right\}^{-1}$$
$$r_{2,t} = \left\{\frac{1}{r_{2,k}} + \frac{M_{CO}}{r_{2,m}}\right\}^{-1} \quad (20)$$
$$r_{3,t} = \frac{r_{3,m}}{M_{H_2}}$$

In the model equations, diffusion terms have been included for the sake of generality. Dimensions of the integration cells are too big to adequately incorporate diffusion terms. Adjusting the size of the integration grid to calculate diffusion in a thermal cracking furnace, would lead to excessive use of computer time and memory.

2.4 Simulation model for the cracking tube

The simulation of the cracking tube with internal helicoidal fins requires the simultaneous integration of the flow equations and the set of continuity equations for all process gas species. The classical, one dimensional flow model no longer gives satisfactory results. Therefore, a full 3D model is used, similar to the one applied for the calculation of the flue gas flow pattern (De Saegher *et al*, 1996).

In the energy Equation, no radiation terms were considered.The reaction kinetics are expressed in terms of the radical reaction scheme CRACKSIM developed at *the Laboratorium voor Petrochemische Techniek* after theoretical developments and extensive pilot experimentation. For the cracking of light hydrocarbons, CRACKSIM contains 1200 elementary reaction steps between 128 species. For each volume element, a stiff set of 128 continuity equations has to be solved.

3 INTEGRATION PROCEDURE

3.1 Coupled simulation of furnace and reactor

The calculation of the heat transfer from the radiation section towards the reactor tube requires a coupled simulation of furnace and reactor. For this purpose, the furnace is divided into a number of isothermal zones. The zone temperatures and the heat fluxes towards the reactor process gas are initially estimated. The energy balances (1) for all zones are solved by using a Rosenbrock method implemented in the software code FURNACE developed at the *Laboratorium voor Petrochemische Techniek*. Next, resulting improved heat fluxes from the furnace to the reactor are used in the reactor tube simulation, yielding improved product yield and temperature profiles. From the heat fluxes, improved external tube

skin temperatures can be calculated. These are used to adapt the energy balances. This iteration has to be repeated until convergence is reached.

3.2 Determination of the flue gas flow pattern

To construct the energy balances for the gas zones, the exchange of flue gas between the different zones has to be known. The flue gas flow pattern is calculated with the software package FLOWSIM developed at the *Laboratorium voor Petrochemische Techniek*. The Reynolds averaged Navier-Stokes Equations are solved together with an energy balance and a turbulence model by using the finite volume technique.

A first order flux difference splitting technique is applied to the convective part of the equations and a central difference scheme for the viscous part (De Saegher *et al.*, 1996). The three dimensional integration grid consists of prims constructed by connecting two dimensional, unstructured grids. The local radiative heat exchange between the different volume elements is calculated from the De Marco-Lockwood flux model.

3.3 Determination of the flue gas concentration profiles

Knowledge of the local flue gas composition is required to calculate both the heat release by combustion in each flue gas volume element and the absorption coefficients for radiation. The concentration profiles are obtained by solving the continuity equations for all flue gas components in each volume element.

3.4 Outline of the calculations

An outline of the calculations is shown in Figure 2. First, the 3D grid for the flow calculations has to be constructed and the furnace has to be divided into volume and surface zones. The view factors for radiation between zones are calculated by means of a Monte Carlo method. All temperatures, the flue gas flow pattern, the flue gas concentration profiles and the heat fluxes from the furnace to the reactor are initially estimated.

From the calculation of the flue gas concentration profiles and the flue gas flow pattern, the input data for a coupled furnace-reactor simulation are obtained. Whereas the global radiative heat transfer from the furnace to the reactor is calculated by the more accurate zone method proposed by Hottel and Sarofim, the local influence of radiative heat transfer is taken into account by the De Marco-Lockwood model, especially designed for short-distance radiative heat transfer.

In the latter model, the tube skin and furnace wall temperatures are considered as fixed boundary conditions. After a coupled simulation of furnace and reactor, improved tube skin and furnace wall temperatures are obtained. Iteration is repeated until these temperatures do no longer vary between two iteration steps.

4 SIMULATION OF THE PROPANE CRACKING UNIT WITH A VERY SHORT RESIDENCE TIME OF THE PROCESS GAS IN THE REACTOR

4.1 Furnace geometry and grid construction

The furnace contains 160 straight reactor tubes on a single row. Each tube makes one pass through the furnace. After the radiation section, the process gas flows through an adiabatic connection, uniting four reactor tubes, before reaching the quenches. The radiation section of the furnace is heated with 40 burners positioned in the bottom plate. The flow pattern is calculated for one of the 40 flames as illustrated in Figure 3 to reduce the computational effort.

Figure 4 shows a top view of this volume element. A two dimensional cross section of the three dimensional integration grid is shown in Figure 5. The three dimensional grid consists of 30 080 irregular prisms constructed by connecting two dimensional grids.

Figure 6 shows the division of the furnace into zones for the coupled simulation of furnace and reactor. Because of symmetry, only one fourth furnace has to be considered, containing 40 gas volume zones, 68 furnace wall zones and 400 reactor tube zones. A cross section of the three dimensional grid for the reactor tube is shown in Figure 7.

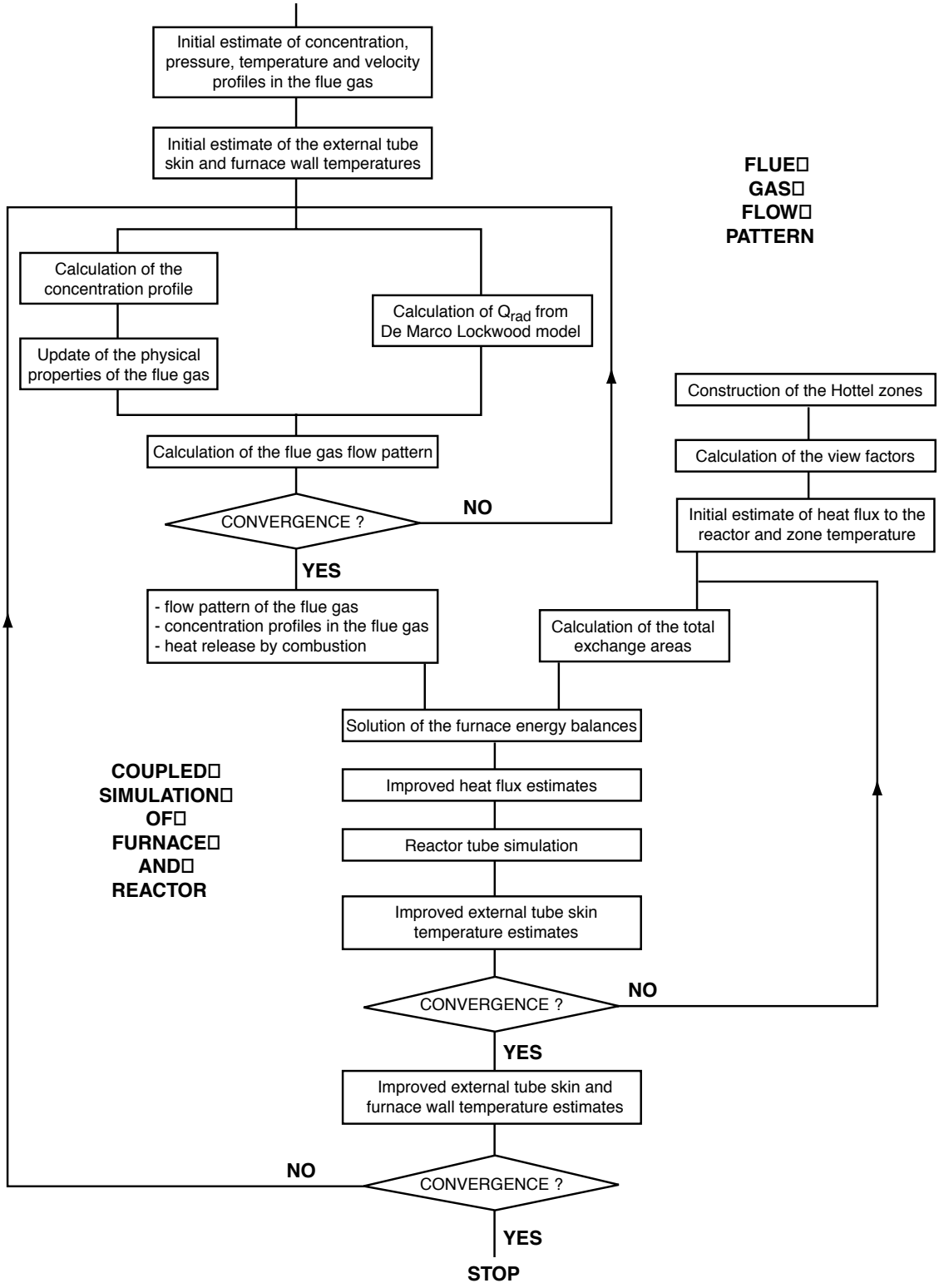

Figure 2

Outline of the calculations.

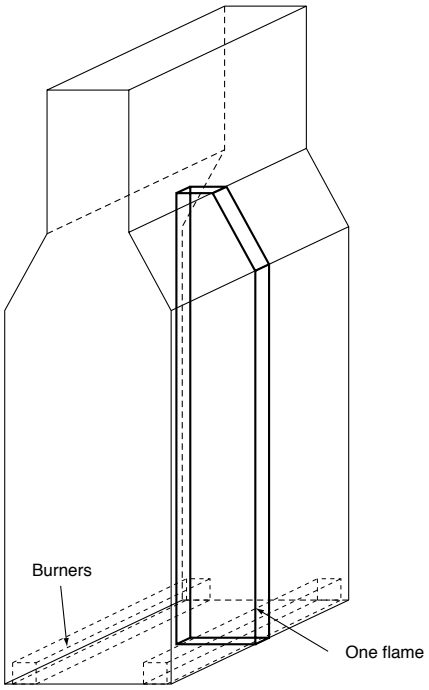

Figure 3

Furnace volume element considered for the calculation of the flue gas flow.

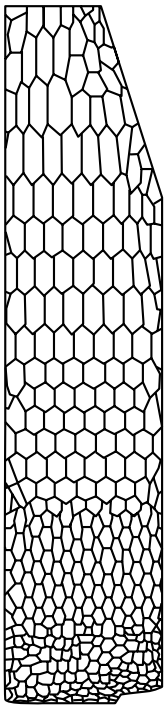

Figure 5

Non-structured, two dimensional cross section of the furnace integration grid.

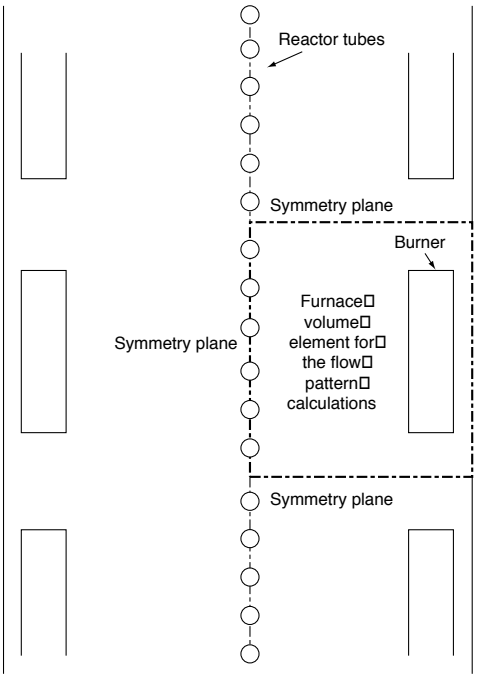

Figure 4

Top view of the furnace volume element for the calculation of the flue gas.

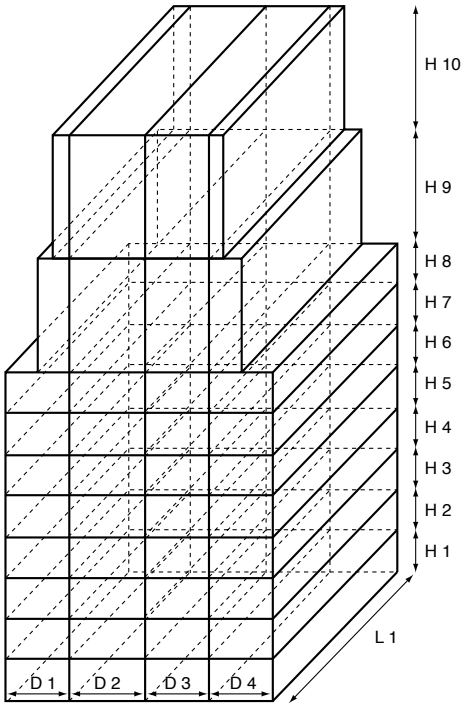

Figure 6

Division of the furnace into Hottel zones.

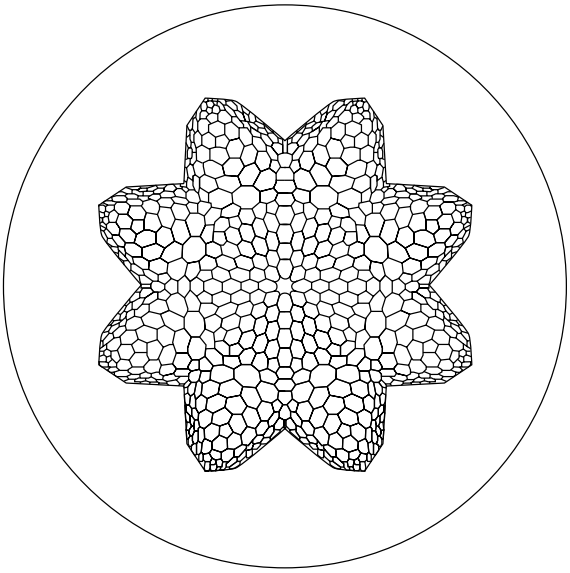

Figure 7

Non-structured, two dimensional cross section of the tube integration grid.

4.2 Simulation results

The calculated velocity vectors in the flue gas are given for different horizontal furnace sections in Figure 8. The stream lines in a vertical section, based on the projected velocity vectors, are shown in Figure 9. Large recirculation patterns, specified by the designer, do not occur.

By assuming these recirculation patterns, the designer underestimated significantly the thermal efficiency of the firebox. This means that the furnace has to be fired harder, resulting in higher tube skin temperatures and short run lengths observed in the industrial unit of this type.

Figure 10 shows the the residual methane percentage in the flue gases. Although 50% of the methane is consumed directly above the burner, a significant amount is burnt higher in the furnace and the observed long flames are observed. The heat flux from the furnace towards the process gas is shown in Figure 11.

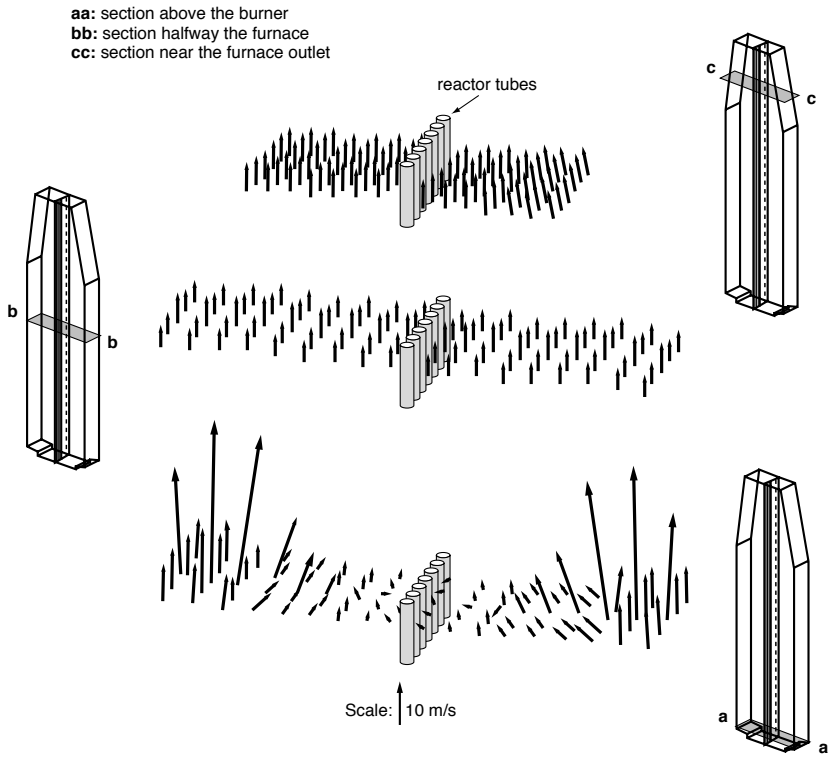

Figure 8

Velocity vectors in two dimensional furnace sections at several heights.

The heat fluxes have been averaged over all reactor tubes, since no significant differences occurred among them. Figure 12 shows the velocity vectors in a cross section of the reactor tube at 4 m from the reactor inlet.

The propane conversion profile averaged over all the reactor tubes is shown in Figure 13. The simulation of the adiabatic connection and the primary quench can not be omitted, since 5% of the propane is converted there.

Figure 14 shows the methane, ethylene and propylene yields through the reactor. The tube skin temperatures and the process gas temperature are shown in Figure 15. Figure 16 shows isotherms in a cross section of the reactor tube at 4 m from the reactor inlet. In the core of the tube, temperature gradients are whiped out due to turbulent mixing.

In the valleys of the fins, steep temperature gradients occur. From the process gas composition and the internal tube skin temperature, the initial coking rate can be calculated. The thermal cracking of hydrocarbons is always accompanied by coke formation, fouling the internal tube skin. This hampers the heat transfer gas and reduces the diameter, increasing the pressure drop over the reactor. Coke is formed at the wall, initially by catalytic mechanisms associated with the surface composition of the tube alloy.

In a later stage, coke grows through addition of unsaturated components to radical positions in the macroradical coke (Froment, 1990) leading to an asymptotic rate.

Figure 17 shows the circumferentially averaged initial coking rate profiles, calculated from a rate equation developed at the *Laboratorium voor Petrochemische Techniek* after extensive pilot experimentation.

Figure 18 shows the circumferential distribution of this coking rate. The high coking rates inside the fin valleys cause a rapid filling of these valleys which is detrimental for the heat transfer. These results were in excellent agreement with the industrial observations.

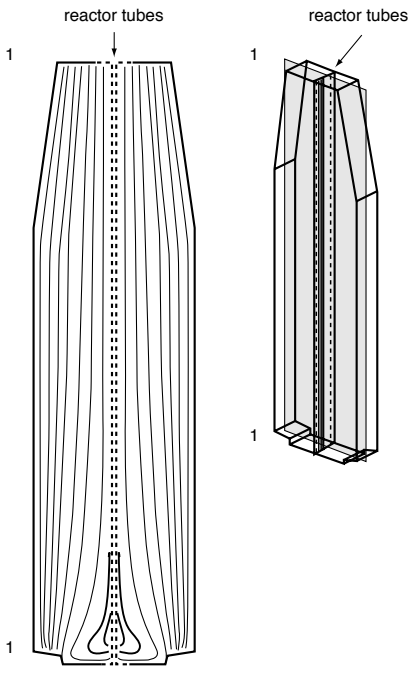

Figure 9

Stream lines in a cross section based on projected velocity vectors.

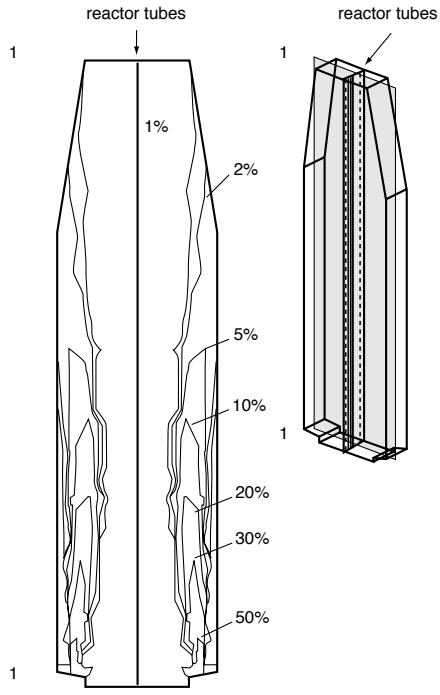

Figure 10

Residual methane percentage in a two dimensional furnace section.

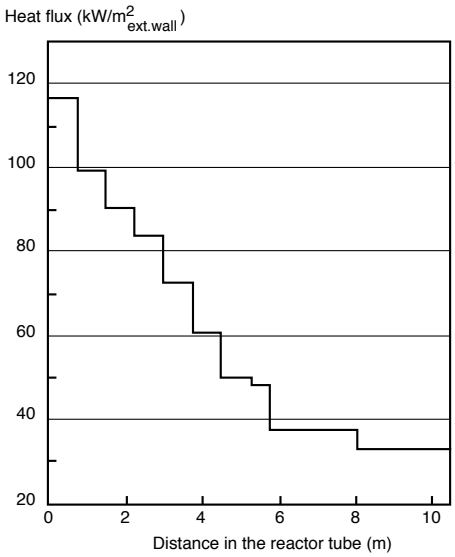

Figure 11

Heat flux flue gaz-process gas averaged over all the reactor tubes.

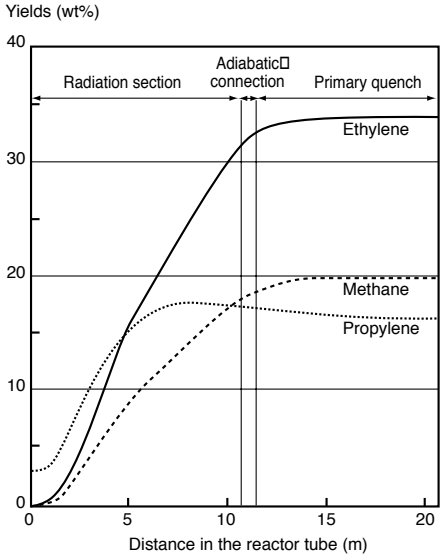

Figure 14

Methane, ethylene and propylene yields averaged over all reactor tubes.

Figure 12

Velocity vectors in a cross section of the reactor tube at 4 m from the reactor.

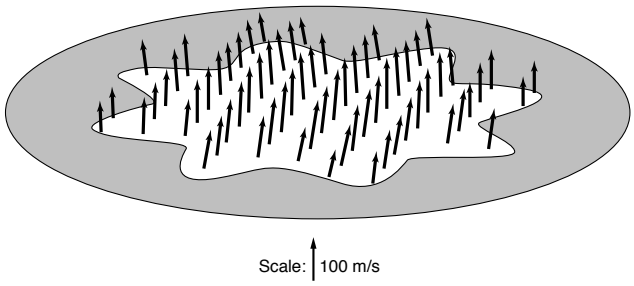

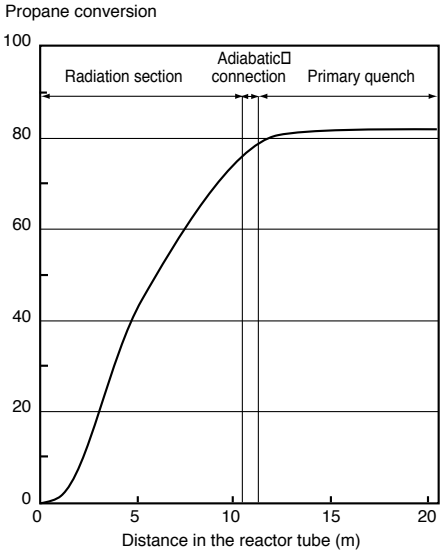

Figure 13

Propane conversion profile averaged over all reactor tubes.

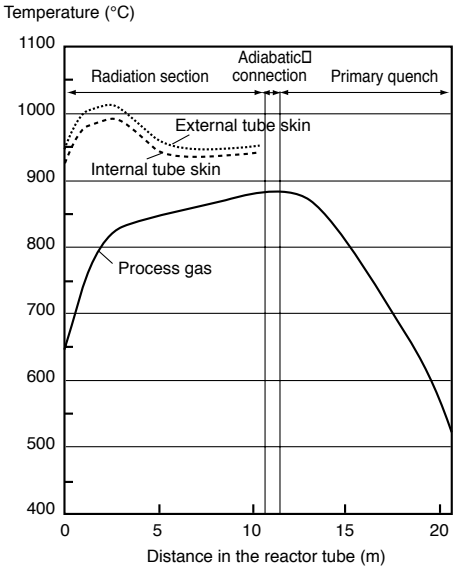

Figure 15

Temperature profiles averaged over all reactor tubes.

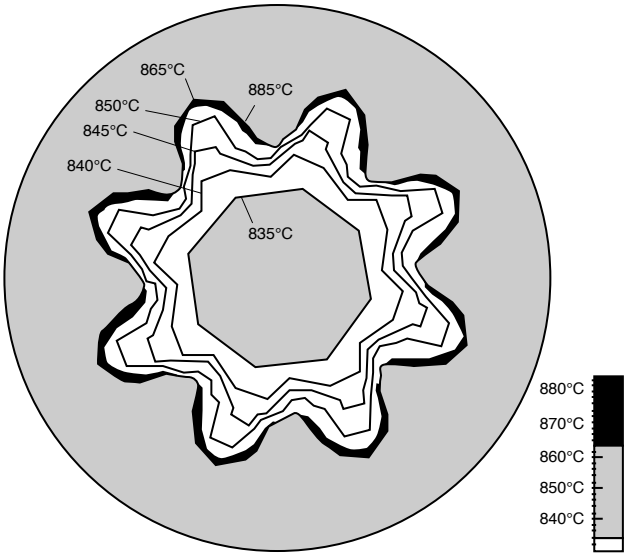

Figure 16

Isotherms in a cross section at 4 m from the reactor inlet.

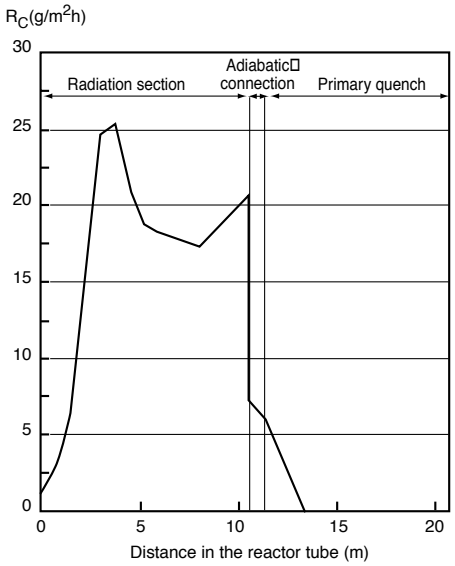

Figure 17

Initial coking rate profile averaged over all reactor tubes.

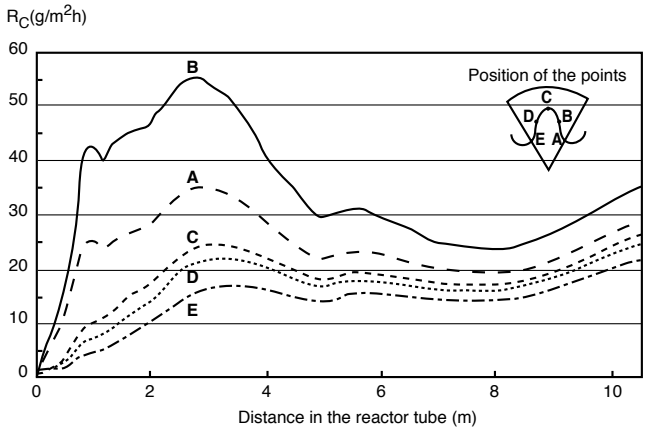

Figure 18

Initial coking rate profiles for several points of a cross section of the tube.

5 COMPUTATION TIME

The simulation of the propane cracking unit was carried out on an IBM RISC 6000 machine (model 375) and took approximately 800 CPU hours. With the actual evolutions in computer technology, this will be reduced considerably in the near future.

CONCLUSION

A procedure was discussed for the simulation of an industrial propane cracking unit with a very short residence time of the process gas in the reactor. A full, three dimensional computational fluid dynamics model was used for the simulation of both the firebox and the reactor tube with internal helicoidal fins.

The firebox simulation revealed that no large recirculation patterns occur in the flue gas. By assuming these recirculation patterns, the designer overestimated the thermal efficiency of the firebox, explaining the industrial problems observed with these units.

The reactor simulation revealed severe temperature gradients in the valleys of the fins. The coke formation was also simulated. Circumferential profiles were pronounced. Local values of the coking rate can be

twice as high as the circumferentially averaged values. This leads to a rapid filling of the fin valleys, which is detrimental for the heat transfer. For this type of units, the adiabatic connection and the primary quench have to be incorporated in the simulation since up to 5% of the propane conversion is achieved there.

NOTATION

C_j	concentration of species *j*	mol cm^{-3}
C_p	specific heat at constant pressure	J kg^{-1} K^{-1}
C_{pj}	C_p of species *j*	J kg^{-1} K^{-1}
D_m	molecular diffusivity	m^2 s^{-1}
D_{turb}	turbulent diffusivity	m^2 s^{-1}
D_t	sum of D_m and D_{turb}	m^2 s^{-1}
e_k	specific kinetic energy	J kg^{-1}
E	blackbody emissive power	J m^{-2} s^{-1}
H	total enthalpy	J kg^{-1}
H_j	enthalpy of formation of species *j*	J kg^{-1}
$-DH_i$	heat of reaction *i*	J kg^{-1}
k	turbulent kinetic energy	J kg^{-1}
k_g	radiation absorption coefficient	m^{-1}
M_j	molecular weight of species *j*	kg mol^{-1}
M_m	molecular weight of the gas mixture	kg mol^{-1}
p	pressure	Pa
R_j	rate of formation of component *j*	mol m^{-3} s^{-1}
$r_{i,k}$	rate of reaction *i*	mol m^{-3} s^{-1}
$r_{i,m}$	mixing rate for reaction *i*	kg m^{-3} s^{-1}
T	temperature	K
U_i	velocity component in the *i*-direction	m s^{-1}
x_i	coordinate in the *i*-direction	m
y_j	weight fraction of component *j* in the gas mixture	-
Z_iZ_j	total exhange area between zones *i* and *j*	m^2

GREEK SYMBOLS

ε	dissipation of turbulent kinetic energy	m^2 s^{-3}
λ_m	molecular conductivity	J m^{-1} s^{-1} K^{-1}
λ_{turb}	turbulent conductivity	J m^{-1} s^{-1} K^{-1}
λ_t	sum of λ_m and λ_{turb}	J m^{-1} s^{-1} K^{-1}
μ_m	molecular viscosity	Pa s
μ_{turb}	turbulent viscosity	Pa s
μ_t	sum of m_m and m_{turb}	Pa s
ρ_g	density	kg m^{-3}

REFERENCES

De Marco A.G. and Lockwood F.C. (1975) A new flux model for the calculation of radiation in furnaces. *La Rivista dei Combustibili*, 29, 184.

De Saegher J.J., Detemmerman T. and Froment G.F. (1996) Three dimensional simulation of high severity internally finned cracking coils for olefins production. *La Revue de l'Institut français du pétrole*, 51, 245-260.

Froment G.F. (1990) Coke formation in the thermal cracking of hydrocarbons. *Reviews In Chem. Eng.*, 6, 294-328.

Hinze J.O. (1959) *Turbulence; An Introduction to its Mechanisms and Theory*, McGraw-Hill, New York.

Hottel H.C. and Sarofim A.F. (1967) *Radiative Transfer*, Mc Graw-Hill, New York.

Plehiers P.M. and Froment G.F. (1989) Firebox Simulation of Olefin Units. *Ind. Eng. Commun.*, 80, 81.

Rao M.V.R., Plehiers P.M. and Froment G.F. (1988) The coupled simulation of heat transfer and reaction in a pyrolysis furnace. *Chem. Eng. Sci.*, 43, 1223.

Spalding D.B. (1972) *Mixing and Chemical Reaction in Steady Confined Turbulent Flames*, Imperial College of Science and Technology, London, 649.

Vercammen H.A.J. and Froment G.F. (1978) Simulation of thermal cracking furnaces. *ACS Symp. Ser., No. 65, Chemical Reaction Engineering*, V.W. Weekman and D. Luss, eds., 271-281.

Vercammen H.A.J. and Froment G.F. (1980) An improved zone method for the simulation of radiation in industrial furnaces. *Int. J. Heat Transf.*, 23, 329.

Willems P.A. and Froment G.F. (1988a) Kinetic modeling of the thermal cracking of hydrocarbons. 1. *Calculation of Frequency Factors', Ind. Eng. Chem. Res.*, 27, 1958-1966.

Willems P.A. and Froment G.F. (1988b) Kinetic modeling of the thermal cracking of hydrocarbons. 2. *Calculation of Activation Energies', Ind. Eng. Chem. Res.*, 27, 1966-1971.

Final manuscript received in February 1998